

# SRF LEVITATION AND TRAPPING OF NANOPARTICLES\*

R. L. Geng<sup>†</sup>, ORNL, Oak Ridge, Tennessee, USA  
P. Dhakal, B. Kross, F. Marhauser, J. McKisson, J. Musson,  
H. Wang, A. Weisenberger, W. Xi, JLab, Newport News, Virginia, USA

## Abstract

A proposal has been conceived to levitate and trap mesoscopic particles using radio frequency (RF) fields in a superconducting RF (SRF) cavity. Exploiting the intrinsic characteristics of an SRF cavity, this proposal aims at overcoming a major limit faced by state-of-the-art laser trapping techniques. The goal of the proposal is to establish a foundation to enable the observation of quantum phenomena of an isolated mechanical oscillator interacting with microwave fields. An experiment supported by LDRD funding at JLab has started to address R&D issues relevant to these new research directions using existing SRF facilities at JLab. The success of this experiment would establish its ground-breaking relevance to quantum information science and technology, which may lead to applications in precision force measurement sensors, quantum memories, and alternative quantum computing implementations with promises for superior coherence characteristics and scalability well beyond the start-of-the-art. In this contribution, we will introduce the proposal and basic considerations of the experiment.

## INTRODUCTION

While levitation and trapping have always attracted attention and found applications such as for containerless processing and spectroscopy of microparticles [1], recent developments in the field of optomechanics have brought about levitation of nanoparticles enabling observation of quantum phenomena in the context of quantum science and technology.

Quantum properties occur when a macroscopic matter particle, being trapped in an optical field and behaving like a mechanical oscillator, is further cooled, either by the same trapping optical field or by an external laser, to its fundamental quantum ground state. Coherent control of a macroscopic quantum system has potentially game-changing implications for fundamental physics as well as technology. It could allow the exploration of the classical-to-quantum boundary, the development of precision force measurement sensors, and could provide a fundamental building block for quantum information [2]. The motion of a “membrane” type mechanical oscillator, embodied by a compliant capacitor in an LC resonator, has been demonstrated to entangle with a propagating electrical signal, with one half of the entangled state being stored in the mechanical oscillator [3]. That result highlighted the potential for the mechanical oscillators to serve as quan-

tum memories for microwave signals and to allow information retrieval from the memory on demand.

Levitated nanoparticles offer the unique and appealing feature of being highly decoupled from the environment, allowing the observation of extremely high quality factors (theoretically expected up to  $10^{12}$ ) in a mechanical oscillator. As the main source of heating is avoided by being free from mechanical attachment to other mechanical objects, reaching the quantum ground state of the mechanical motion of levitated particles is hence greatly facilitated. Recent experiments obtaining optical trapping of a dielectric silica sphere of  $\sim 140$  nm in diameter at ambient temperature in vacuum, have demonstrated the realization of the quantum ground state [4, 5].

Four current challenges are identified for nanoparticle trapping and cooling with light fields in an optical cavity [6]: (1) stable trapping at high vacuum; (2) minimizing the mechanical occupation; (3) minimizing the photon shot noise; (4) maximizing the optomechanical coupling.

We proposed an experiment on levitation and trapping mesoscopic particles by RF fields in an SRF cavity, SRF levitation and trapping of nanoparticles, aimed at enabling the ultimate observation of quantum phenomena in the context of quantum science and technology. Our approach is expected to bring a new tool that is unfamiliar to the field of optomechanics. Most critically, by virtue of much longer wavelength (factor of  $10^5$ ), ultra-high vacuum (down to  $10^{-10}$  -  $10^{-11}$  mbar), and cryogenic temperatures (1-4 K), it addresses three of the four currently identified challenges faced by optomechanical nanoparticle levitation, therefore promises to advance nanoparticle levitation well beyond the state of the art demonstrated by optical cavities. Expected gains in other metrics:

- ◆ Photon scattering,  $P_{scat} = |\alpha|^2 k_L^4 J_{opt}^2 / 6\pi\epsilon_0^2$ , to be reduced by  $10^{20}$ .
- ◆ Mechanical phonon occupation,  $n_m = k_B T_{env} / h\omega_q$ , to be reduced by  $10^2$ .
- ◆ Cavity internal loss  $k_{cav}$  to be reduced by a factor of  $10^4$ .

## SRF LEVITATION AND TRAPPING

### Theory

The gradient force is the major driving force behind the SRF levitation and trapping. Such a force arises in an EM field where a spatial variation in the field amplitude, electric or magnetic, exists. For a dielectric particle in air or vacuum, in the Rayleigh regime where the particle radius,  $r$ , being sufficiently smaller than the wavelength of the electromagnetic field  $\lambda$ ,  $r < \lambda/20$ , the time-averaged gradient force arises from spatial variation of the electric field amplitude,

\* Authored by UT-Battelle, LLC, under contract DE-AC05-00OR22725 with the US Department of Energy and by Jefferson Science Associates, LLC under U.S. DOE Contract No. DE-AC05-06OR23177

<sup>†</sup> gengr@ornl.gov, formerly with JLab.

Content from this work may be used under the terms of the CC BY 4.0 licence (© 2022). Any distribution of this work must maintain attribution to the author(s), title of the work, publisher, and DOI

$$F_{grad,e} = \frac{1}{4} \alpha \nabla E(\vec{r})^2, \quad (1)$$

where  $\alpha$  is the polarizability of particle,

$$\alpha = 4\pi r^3 \epsilon_0 \frac{\epsilon_r - 1}{\epsilon_r + 2}. \quad (2)$$

Herein  $\epsilon_0$  is the permittivity of vacuum, and  $\epsilon_r$  is the relative permittivity of the particle.

Other forces involved are the gravitational force and the photon scattering force,

$$F_g = mg = \frac{4\pi}{3} \rho g r^3, \quad (3)$$

$$F_{scat}(\vec{r}) = \frac{\sigma_s \langle S(\vec{r}, t) \rangle_T}{c}, \quad (4)$$

where  $m$  is the mass of the particle,  $g$  the gravity constant,  $\rho$  the density of the particle,  $c$  the speed of light in vacuum,  $\langle S(\vec{r}, t) \rangle_T$  the time-averaged Poynting's vector.  $\sigma_s$  is the scattering cross-section,

$$\sigma_s = \frac{8}{3} \pi k^4 r^6 \left( \frac{\epsilon_r - 1}{\epsilon_r + 2} \right)^2, \quad (5)$$

where  $k = 2\pi/\lambda$  is the wave number in vacuum. The scattering force is insignificant in the context of particle trapping, but is important for cooling the mechanical motion of a trapped particle, an ultimate goal toward the demonstration of our idea's relevance to QIS.

### Analytical Result of Levitation & Trapping in an Elliptical Cavity Excited in $TM_{010}$ Mode

Figure 1 illustrates a single-cell 1.3 GHz TESLA shape cavity with a dielectric particle levitated and trapped in the electric field of the  $TM_{010}$  mode. The trapping force is directed toward the center of the cavity where  $E(\vec{r})^2$  has a local maximum. The gravity force  $F_g$  is balanced by the axial trapping force  $F_{trap,z}$ , together with radial trapping force  $F_{trap,r}$ .

In using a fused silica sphere as an example (the popular particle used in laser trapping, the particle parameters: relative permittivity  $\epsilon_r = 2.2$ ; particle mass density  $\rho = 2650 \text{ kg/m}^3$ ) we demonstrate levitation is achievable with modest cavity RF fields corresponding to an accelerating field,  $E_{acc}$ , of 13 MV/m in the  $TM_{010}$  mode. This is a field level easily attainable in today's SRF niobium cavities. For example, the cavity G2, a single-cell TESLA end cell shape cavity, reached a maximum  $E_{acc} = 40 \text{ MV/m}$  with high unloaded quality factor values [7]. Only 1 W of RF power dissipation is needed to support a gradient of 40 MV/m. In addition, analytical 1D particle tracking with 1D field map shows that optimal trapping can be achieved with hollow dielectric particles.

In summary, our analysis established the access to SRF levitation and trapping with comfortable margins by using modern SRF cavities. Moreover, we have shown that: (1) SRF levitation and trapping of dielectric particles is independent of the particle radius, or uniform trapping insensitive to particle size variation; (2) Tuning the RF field can efficiently adjust the ratio of the trapping force to the gravitational force; (3) Particle size is an effective knob for trapping force allowing a wide range of 60 zN - 60  $\mu\text{N}$  for particle radii within 10 nm to 1 mm. Hence SRF levitation and trapping offer excellent opportunities for sensitive force measurements for quantum-limited sensor development or containerless material purification.

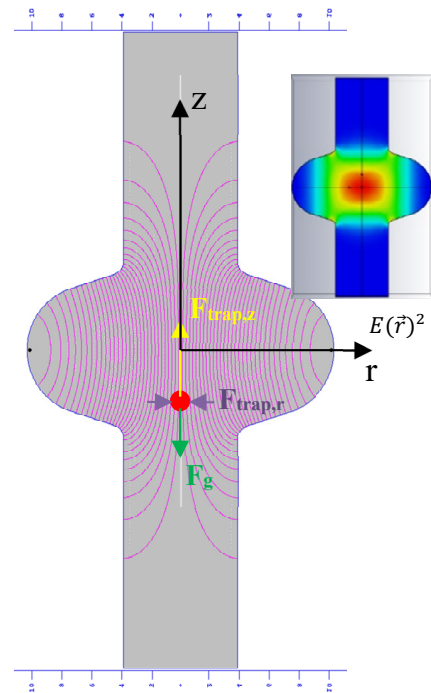


Figure 1: Sketch of levitated dielectric particle. Inset: contour map  $E(\vec{r})^2$  of  $TM_{010}$  mode.

### Experimental Considerations

Figure 2 illustrates a sketch of the experimental elements, including an SRF cavity driven by a phase-locking circuit, a particle delivery device that may also serve as a light source for particle illumination, a high-speed camera, and possibly a laser interferometer for quantitatively assessing the particle oscillation amplitude.

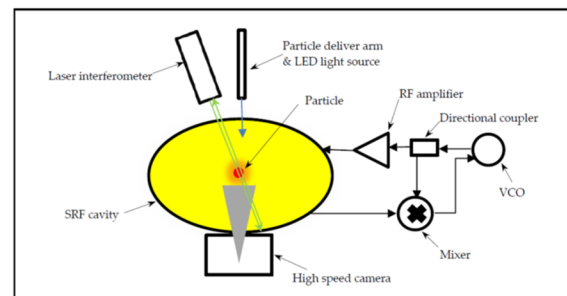


Figure 2: Schematic experimental apparatus.

## PARTICLE DELIVERY

### Thin Tube Penetrating the Cavity Space

An existing 1.3 GHz SRF cavity has been identified at JLab – designed by DESY – that was chosen for the first experimental proof-of-principle RF levitation study. It is a 1.5-cell cavity (see Fig. 3) previously used for photo-injector gun cavity R&D. The cavity back wall features a small hole at its center. The back wall is mechanically stiffened and carries a flange that nominally allows the installation of a photocathode plug, which can be sealed with indium to the back wall. For our case, the cavity will

be re-purposed to insert a thin niobium tube instead of a photocathode plug. The aim is to preload the tip of the tube with dielectric particulates. The advantage of this configuration is that the tip can be placed close to the theoretical point, where RF levitation of polarized dielectrics would be feasible.



Figure 3: An existing 1.5-cell TESLA shape SRF niobium cavity to be used for the proof-of-principle experiment.

Numerical RF simulations show that the insertion of a metallic tube ( $\bullet = 4.8$  mm) will detune the typical  $TM_{010}$ -like  $\blacktriangle$ -mode in the 1.5 cell cavity so that one can create a  $TM_{010}$ -like mode predominantly resonating in the full cell similar to the RF field in a single-cell cavity.

For instance, Fig. 4 shows the RF electric field contours, when the tube is inserted up to the cavity iris (57.7 mm insertion depth). The RF field in the first half-cell is significantly suppressed. The detuning of the nominal cavity frequency is -5.6 MHz in this case. At the same time, the electric surface peak field on the tip is reduced to a value smaller than on the cavity irises and it is also smaller than the on-axis peak field.

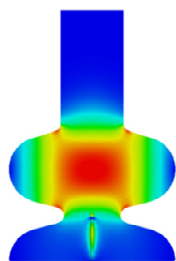


Figure 4: Electrical field contour of the  $TM_{010}$ -like mode in the 1.5 cell cavity being detuned by a metallic tube in the first half-cell. The RF field is now predominantly residing in the full cell.

The concern of potential field-emitted electrons arising from the tip of the tube is therefore reduced. In fact, for an insertion  $\sim 8.7$  mm shy from reaching the iris, the electric field enhancement on the tip can be nearly eliminated. It was found though that this is not the optimal position for RF levitation, and that the tube should be placed slightly into the full cell and thus closer to the ideal levitation point. Note that the unloaded  $Q$ ,  $Q_0$ , of the cavity will actually not degrade due to the presence of the tube but slightly increase ( $\sim +28\%$ ). This is due to the absence

of strong magnetic fields in the first cell, while the magnetic field of a  $TM$  monopole mode is zero along the cavity axis. The RF losses on the tube surface are therefore comparably small. The simulations indicate that the  $Q_0$  associated with the tube alone should be in the lower  $10^{12}$  range and the cavity  $Q_0$  around  $1 \times 10^{10}$ . This presupposes a cooling of the cavity and tube surfaces down to  $\sim 2$  K. This analysis provides some confidence that the cavity  $Q_0$  does not deteriorate drastically even if the temperature of the Nb tube would be slightly elevated since relying purely on thermal conduction to the liquid helium surrounding the cavity.

### Particle Launching

Two options are being developed for particle launching into the trapping volume.

The gas launching method injects particles into the SRF cavity via a thin niobium tube penetrated into the cavity vacuum space. A niobium foil, welded to the end of the tube followed by a short extension, forms a cup at the tip of the tube with a bottom diaphragm. Particles, pre-loaded in the cup, are launched by injecting a pulse of gas helium into the evacuated space underneath the diaphragm. A sketch of this apparatus is shown in Fig. 5.

The acoustic method launches particles by using an ultrasound transducer in contact with the warm end of a niobium tube/rod. The acoustic energy is transferred via the tube/rod to its cold end where particles are pre-loaded. A key figure of merit for particle launching is the vibration velocity of the cold end of the niobium tube/rod. The acoustic frequency is a useful knob for adjusting the particle launching conditions.

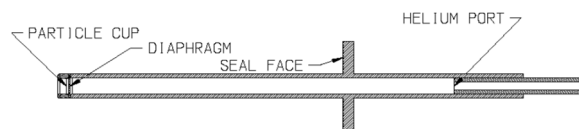


Figure 5: Gas launching apparatus.

### PARTICLE IMAGING AND TRACKING

Optical monitoring within UHV chambers is commonly performed using sophisticated periscope systems, involving many lens and prism assemblies [8]. Since RF cavity studies prevent the use of windows or orifices on the structures, proximity to the experiment is an issue, especially when considering the complexity of objective lens design [9]. As an alternative, the use of a borescope/ endoscope has been considered for this study, providing several attractive features, including a minimally invasive aperture to the RF field, intrinsic illumination, self-contained structure, and, unlike microscope objectives, the magnification is not fixed, but it is dependent on the working distance. As a result, the scope has a very long depth-of-field (DoF), providing magnification of 1 for centimeter distances, up to 25 for millimeter distances. A DoF of  $\sim 10$  cm permits the optical elements to be completely removed from the RF cavity (and associated fields), while also avoiding thermal contact with ultracold niobium structures.

Content from this work may be used under the terms of the CC BY 4.0 licence (© 2022). Any distribution of this work must maintain attribution to the author(s), title of the work, publisher, and DOI

Conventional endoscopes consist of an optical objective, followed by a relay section designed to carry the image to the ocular element. In a conventional Hopkins relay, discrete lens and glass rod lattices alternately focus and de-focus the image along the extent of the rigid pipe [10]. A newer development known as GRIN glass fiber allows a single fiber's index of refraction to be radially modulated, providing continuous lensing, as well as correction for chromatic aberrations [10,11]. The particular endoscopic system is a rigid 29 cm industrial unit, having a 4.8 mm diameter, and an overall length of 29 cm. While not explicitly guaranteed by the vendor, discussions with applications engineers indicate that the device is UHV compatible, and able to withstand liquid-nitrogen temperatures. Since the SRF cavity requires ~4K temperature, care will be taken to isolate (but not eliminate) colder temperatures for optical and electrical camera equipment. Figure 6 depicts the general schematic of Hopkins and GRIN relay systems, as well as the dimensions particular to the instrument used in this study. The specifications for the endoscope are presented in Table 1.

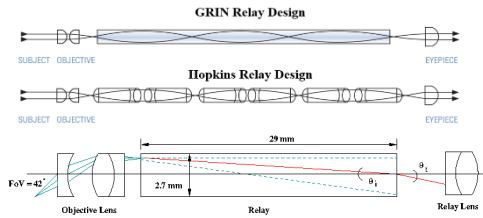


Figure 6: Schematic of endoscopic relay section, comparing the discrete-element Hopkins system with the continuous gradient index (GRIN) design. The dimensions pertaining to the unit for our study are given in the lower figure and used for resolution calculations. In both cases, the objective lens is usually integrated into the first few mm of the endoscope.

Table 1: Endoscope Characteristics

Optical Parameter	Quantity
Direction of View (DoV)	0°, 90°
Full Field of View (FoV)	42°
Endoscope Diameter	4.2 mm (4.8 mm w/ prism)
Clear Aperture	2.7 mm
Entrance Pupil Diameter ( $D_e$ )	0.56 mm
Endoscope Length ( $l$ )	29 cm
Wavelength ( $\lambda$ )	538 nm
Working Distance ( $d$ )	1 cm < $d$ < 10 cm
Resolution, $r(d)$	8 lp/mm < $r(d)$ < 85 lp/mm

To observe and record the dynamic behavior of the levitated microspheres, a Krontech Chronis 2.1 high-speed camera was selected. In addition to an attractive price point, the system is capable of full-resolution (1980x1280) shutter speeds of 1000 frames per second (fps), while providing up to 100,000 fps for the lowest resolutions (1920x8) [12]. The system is capable of exter-

nal control for triggering, high-speed streaming, Ethernet control (via on-board web server), and 11 seconds of recording using 32 GB of on-board memory.

It is estimated that, without magnification, the resolution of the endoscope assembly is consistent with that of the camera sensor, provided there is ample contrast. A standard C-mount adapter (75 mm focal length) is used to mate the optics with the camera, providing additional optical magnification, ensuring the ability to see the ~100-300  $\mu$ m spheres, with reasonable contrast.

Lighting is provided by a Luxxor 35W LED source, with a flexible light guide. Since the system is modular, the expected use of filters should permit the optimization of contrast, as well as facilitate the possible use of UV for fluorescent-coated spheres. Other illumination options include laser light, for which specific wavelengths can be used (eg. 355 nm for UV).

## PLAN FOR EXPERIMENTS

The proof of principle cryogenic experiment will be conducted in an existing vertical Dewar at JLab's cavity testing facility. The cavity assembly with the particle delivery system and imaging configuration will be submerged into liquid helium at 2 K. The imaging configuration will be isolated with liquid helium with the enclosure maintained at room temperature above the cavity flange. The cavity RF power will be controlled to reach the optimal gradient in CW operation. Once the cavity ramps to its desired electric field, the dielectric particles will be launched with the mechanism described above. The continuous monitoring of the phase, resonant frequency and quality factor of the cavity allows us to probe the interaction of the levitated particles and RF field.

## CONCLUSION

In conclusion, a proposal has been conceived to levitate and trap mesoscopic particles using RF fields in an SRF cavity, aimed at establishing a foundation to enable observation of quantum phenomena of an isolated mechanical oscillator interacting with microwave fields.

An experiment supported by LDRD funding at JLab has started to address R&D issues relevant to these new research directions using existing SRF facilities at JLab. This experiment, if successful, will establish a platform enabling exploration of an electromechanical system consisting of a trapped macroscopic mechanical oscillator and a superconducting RF resonator, aimed at ultimately generating entanglement between the motion of a trapped particle mechanical oscillator and a propagating microwave field [13]. Such a platform would offer an opportunity for developing qubits with superior scalability as compared to trapped ions due to the large trap volume and coherence time,  $\tau = \hbar\omega_q/k_B T_{bath}$ , up to 10 sec, 3-4 order of magnitude longer than that in the state of art SQUID based quantum computer architecture [14]. In addition, it provides opportunities for developing precision force measurement sensors and testing quantum theory in the macroscopic domain.

## REFERENCES

- [1] E. H. Brandt, "Levitation in physics", *Science*, vol. 243, pp. 349-355, 1989. doi:10.1126/science.243.4889.349
- [2] G. Ranjit, D. P. Atherton, J. H. Stutz, M. Cunningham, and A. A. Geraci, "Attonewton force detection using microspheres in a dual-beam optical trap in high vacuum", *Phys. Rev. A*, vol. 91, p. 051805(R), 2015. doi:10.1103/PhysRevA.91.051805
- [3] T. A. Palomaki, J. D. Teufel, R. W. Simmonds, and K. W. Lehnert, "Entangling mechanical motion with microwave fields", *Science*, vol. 342, pp. 710-713, 2013. doi:10.1126/science.1244563
- [4] F. Tebbenjohanns, M. Frimmer, V. Jain, D. Windey, and L. Novotny, "Motional sideband asymmetry of a nanoparticle optically levitated in free space", *Phys. Rev. Lett.*, vol. 124, p. 013603, 2020. doi:10.1103/PhysRevLett.124.013603
- [5] U. Delić, M. Reisenbauer, K. Dare, D. Grass, V. Vuletić, N. Kiesel, and M. Aspelmeyer, "Cooling of a levitated nanoparticle to the motional quantum ground state", *Science*, vol. 367, pp. 892-895, 2020. doi:10.1126/science.aba3993
- [6] J. Millen, T. S. Monteiro, R. Pettie, and A. N. Vamivakas, "Optomechanics with levitated particles", *Rep. Prog. Phys.*, vol. 83, p. 026401, 2020. doi:10.1088/1361-6633/ab6100
- [7] R. L. Geng, C. Adolphsen, Z. Li, J. K. Hao, K. X. Liu, and H. Y. Zhao, "New results of development on high efficiency high gradient superconducting RF cavities", in *Proc. 6th Int. Particle Accelerator Conf. (IPAC'15)*, Richmond, VA, USA, May 2015, pp. 3518-3520. doi:10.18429/JACoW-IPAC2015-WEPWI013
- [8] B. Rousset, D. Chatain, L. Puech, P. Thibault, F. Viargues, and P-E. Wolf, "Visualization in cryogenic environment: application on two phase studies," *Cryogenics*, vol. 49, no. 10, p. 554, 2009. doi:10.1073/pnas.1312546111
- [9] J.D. Pritchard, J. A. Isaacs, and M. Saffman, "Long working distance objective lenses for single atom trapping and imaging," *Rev. Sci. Instrum.*, vol. 87, p. 073107, 2016. doi:10.1063/1.4959775
- [10] T. Tomkinson, J. Bentley, M.K. Crawford, C. Harkrider, D. Moore, and J. Rouke, "Rigid endoscopic relay systems: a comparative study," *Applied Optics*, vol. 35, no. 34, 1996. doi:10.1364/AO.35.006674
- [11] Gradient Lens Corporation, Rochester, NY. <https://www.gradientlens.com>
- [12] Krontech Corporation, Vancouver, CA. <https://www.krontech.ca/>
- [13] T. A. Palomaki, J. W. Harlow, J. D. Teufel, R. W. Simmonds, and K. W. Lehnert, "Coherent state transfer between itinerant microwave fields and a mechanical oscillator", *Nature*, vol. 495, pp. 210-214, 2013. doi:10.1038/nature11915
- [14] M. Kjaergaard, M. E. Schwartz, J. Braumuller, P. Krantz, J. I-J Wang, S. Gustavsson, and W. D. Oliver, "Superconducting qubits: current state of play", *Annual Review of Condensed Matter Physics*, vol. 11, no. 1, pp. 369-395, 2020. arXiv:1905.13641  
doi:10.1146/annurev-conmatphys-031119-050605